

# An analysis of $h \rightarrow \mu^+ \mu^-$ mode at the center-of-mass energy of 250/500 GeV ILC — part 9

Shin-ichi Kawada

## Abstract

<sup>1</sup> This note is the 9th series of analysis log. Previous notes are in Ref. [1–8]. I will describe new analysis channel: 250 GeV  $\nu\bar{\nu}h$  channel.

---

<sup>1</sup>Release note

• 2017/Nov./6 release

# 1 Introduction

In this note I will describe the analysis of 250 GeV  $e^+e^- \rightarrow \nu\bar{\nu}h$  channel.

## 2 250 GeV $e^+e^- \rightarrow \nu\bar{\nu}h$ analysis: left-handed (nnh250-L)

### 2.1 MC samples

All available SM backgrounds (2f, 4f, 3f, aa\_2f, higgs\_ffh) are used in the analysis. Additionally generated samples which have ELOG [9] ID of 56 - 59 are also included.

### 2.2 Event Reconstruction

I only used IsolatedLeptonTagger [10] for the event reconstruction. The next plots are the distributions of parameters which are used in this processor.

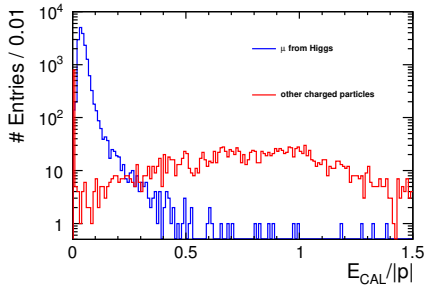


Figure 1:  $E_{CAL}/|p|$  distribution.

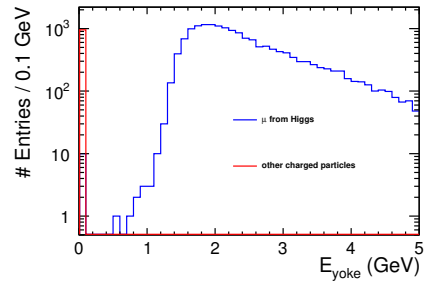


Figure 2:  $E_{yoke}$  distribution.

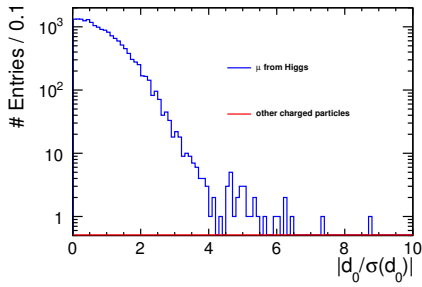


Figure 3:  $|d_0/\sigma(d_0)|$  distribution.

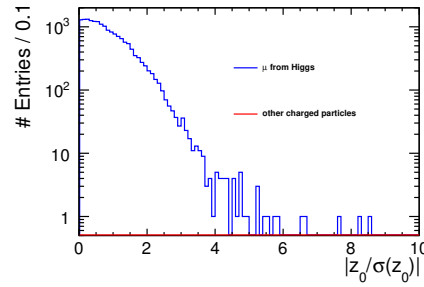


Figure 4:  $|z_0/\sigma(z_0)|$  distribution.

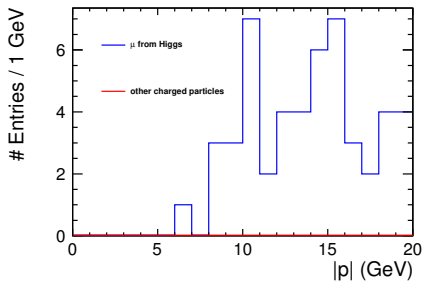


Figure 5:  $|p|$  distribution.

I determined the parameters as following:

- $E_{\text{CAL}}/|p| < 0.3$
- $E_{\text{yoke}} > 0.5 \text{ GeV}$
- $|d_0/\sigma(d_0)| < 5$
- $|z_0/\sigma(z_0)| < 5$
- $|p| > 5 \text{ GeV}$

The reconstruction efficiency (correctly reconstructed one  $\mu^+$  and one  $\mu^-$ ) for the signal sample was 95.8%.

## 2.3 Precuts

I applied following cuts as the precuts.

- exactly one  $\mu^+$  and one  $\mu^-$
- $0.5 < \chi^2/\text{Ndf}(\mu^\pm) < 1.5$
- $|d_0(\mu^\pm)| < 0.02 \text{ mm}$ ,  $|d_0(\mu^-) - d_0(\mu^+)| < 0.02 \text{ mm}$
- $|z_0(\mu^\pm)| < 0.5 \text{ mm}$ ,  $|z_0(\mu^-) - z_0(\mu^+)| < 0.5 \text{ mm}$
- $\sigma(M_{\mu^+\mu^-}) < 0.5 \text{ GeV}$
- $100 < M_{\mu^+\mu^-} < 130 \text{ GeV}$
- $\cos \theta_{\mu^+\mu^-} < -0.4$
- $N_{P_t > 5 \text{ GeV}} = 0$  (charged only)
- $125 < E_{\text{vis}} < 190 \text{ GeV}$
- $40 < M_{\text{rec}} < 140 \text{ GeV}$
- missing  $P_t > 5 \text{ GeV}$
- $|\cos \theta_{\text{miss}}| < 0.99$

Following figures are the distributions of each variable and the table is cut table.

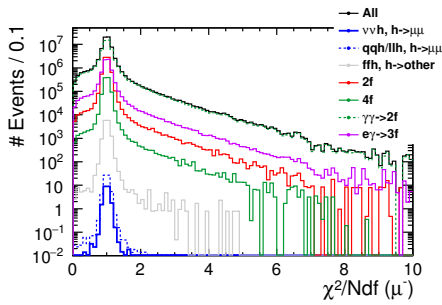


Figure 6:  $\chi^2/\text{Ndf}(\mu^-)$  distribution.

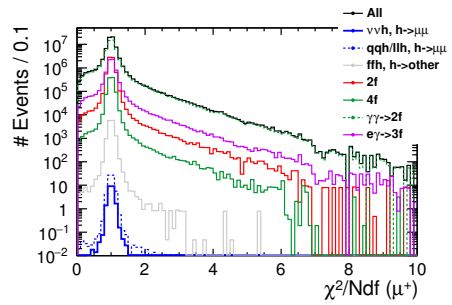


Figure 7:  $\chi^2/\text{Ndf}(\mu^+)$  distribution.

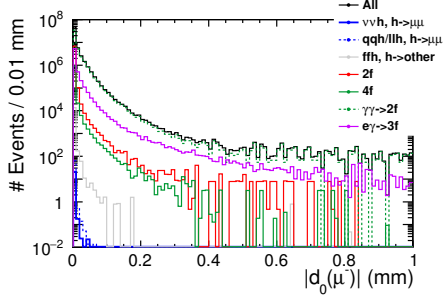


Figure 8:  $|d_0(\mu^-)|$  distribution.

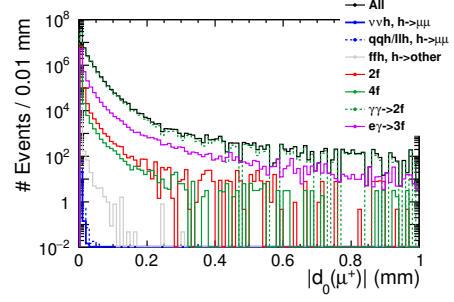


Figure 9:  $|d_0(\mu^+)|$  distribution.

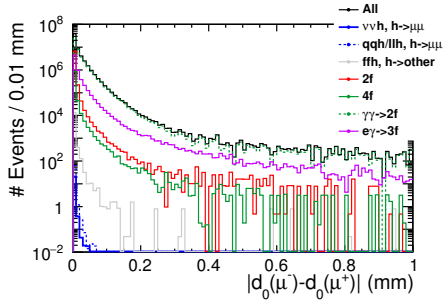


Figure 10:  $|d_0(\mu^-) - d_0(\mu^+)|$  distribution.

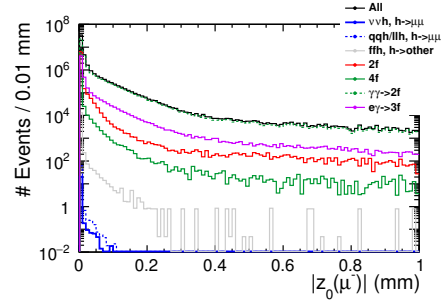


Figure 11:  $|z_0(\mu^-)|$  distribution.

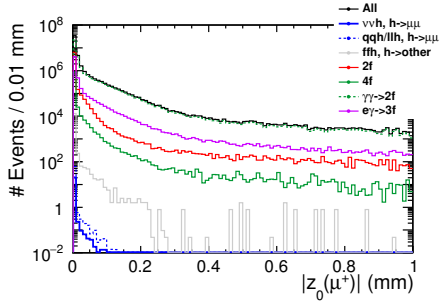


Figure 12:  $|z_0(\mu^+)|$  distribution.

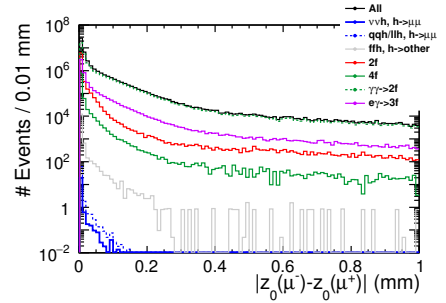


Figure 13:  $|z_0(\mu^-) - z_0(\mu^+)|$  distribution.

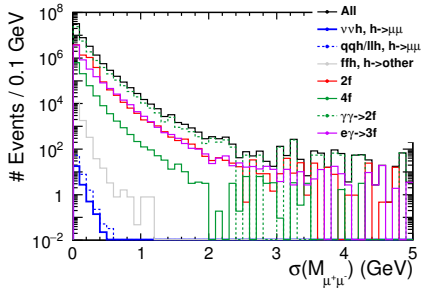


Figure 14:  $\sigma(M_{\mu^+\mu^-})$  distribution.

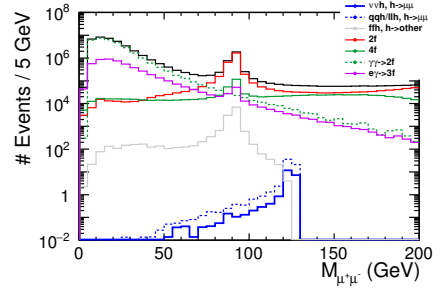


Figure 15:  $M_{\mu^+\mu^-}$  distribution.

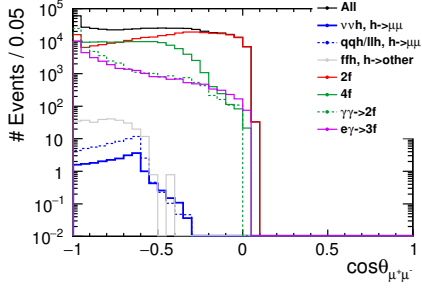


Figure 16:  $\cos \theta_{\mu^+\mu^-}$  distribution.

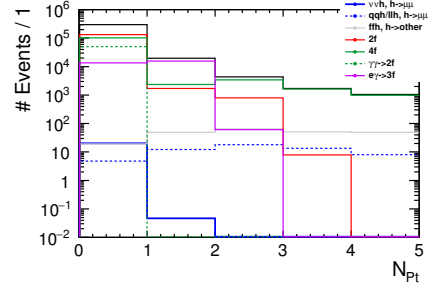


Figure 17:  $N_{P_t > 5\text{GeV}}$  distribution.

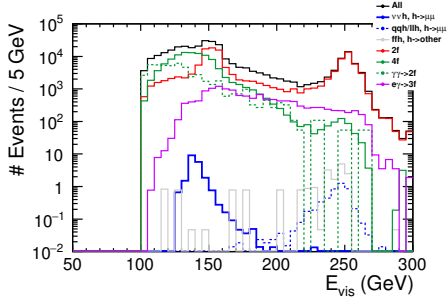


Figure 18:  $E_{\text{vis}}$  distribution.

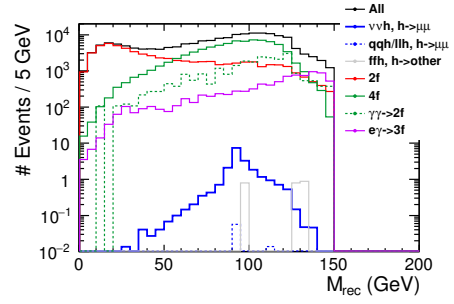


Figure 19:  $M_{\text{rec}}$  distribution.

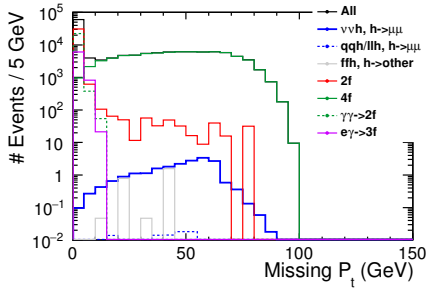


Figure 20: Missing  $P_t$  distribution.

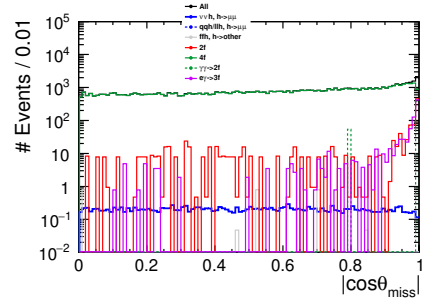


Figure 21:  $|\cos \theta_{\text{miss}}|$  distribution.

Table 1: Cut table of nnh250-L at the precuts.

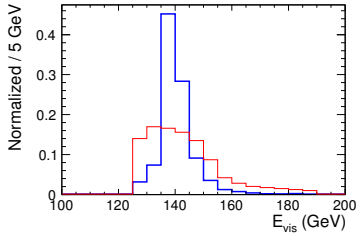
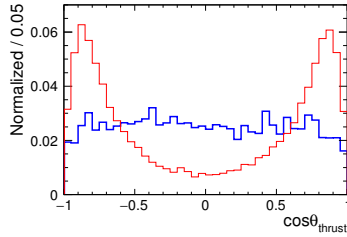
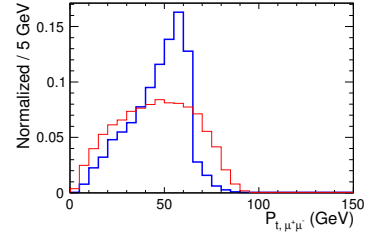
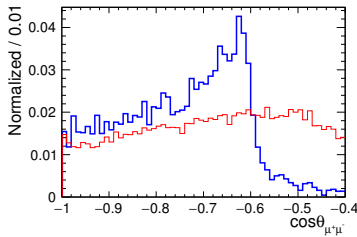
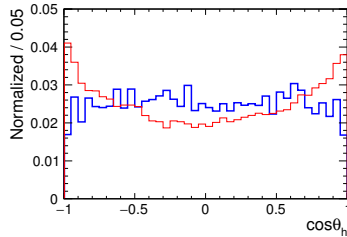
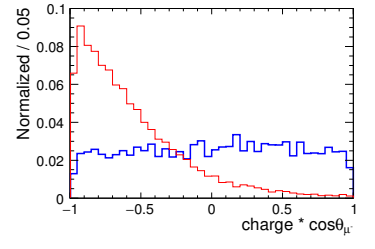
	$\nu\nu h$	$q\bar{q}h+\ell\ell h$	$f\bar{f}h$		2f	4f	$\gamma\gamma \rightarrow 2f$	3f
	$h \rightarrow \mu\mu$	$h \rightarrow \mu\mu$	$h \rightarrow \text{other}$					
No cut	22.55	70.82	$4.311 \times 10^5$	$1.569 \times 10^8$	$5.515 \times 10^7$	$8.925 \times 10^8$	$1.645 \times 10^9$	
# $\mu^\pm$	21.55	64.73	$1.407 \times 10^4$	$7.114 \times 10^6$	$9.854 \times 10^5$	$5.400 \times 10^7$	$7.259 \times 10^6$	
$\chi^2/\text{Ndf}$	21.37	64.04	$1.392 \times 10^4$	$6.893 \times 10^6$	$9.564 \times 10^5$	$4.476 \times 10^7$	$6.351 \times 10^6$	
$d_0$	21.25	63.60	$1.369 \times 10^4$	$6.799 \times 10^6$	$9.265 \times 10^5$	$3.310 \times 10^7$	$5.272 \times 10^6$	
$z_0$	21.23	63.54	$1.368 \times 10^4$	$6.782 \times 10^6$	$9.246 \times 10^5$	$3.263 \times 10^7$	$5.218 \times 10^6$	
$\sigma(M_{\mu\mu})$	21.21	63.50	$1.367 \times 10^4$	$6.658 \times 10^5$	$9.174 \times 10^5$	$3.217 \times 10^7$	$5.111 \times 10^6$	
$M_{\mu\mu}$	20.55	61.73	285.29	$2.793 \times 10^5$	$1.265 \times 10^5$	$5.362 \times 10^4$	$3.244 \times 10^4$	
$\cos\theta_{\mu\mu}$	20.40	61.63	285.29	$1.348 \times 10^5$	$1.121 \times 10^5$	$5.059 \times 10^4$	$2.913 \times 10^4$	
$N_{P_t}$	20.35	4.78	19.16	$1.323 \times 10^5$	$1.030 \times 10^5$	$5.059 \times 10^4$	$1.349 \times 10^4$	
$E_{\text{vis}}$	20.29	0.10	2.46	$7.806 \times 10^4$	$8.082 \times 10^4$	$2.439 \times 10^4$	8792.87	
$M_{\text{rec}}$	20.21	0.10	2.46	$3.223 \times 10^4$	$7.777 \times 10^4$	$2.286 \times 10^4$	6937.62	
missing	20.11	0.10	2.46	1132.23	$7.681 \times 10^4$	431.68	847.30	
$\theta_{\text{miss}}$	20.00	0.10	2.46	683.28	$7.593 \times 10^4$	53.96	425.21	

## 2.4 TMVA Analysis

I used 8 parameters for TMVA analysis as following:

- $E_{\text{vis}}, \cos\theta_{\text{thrust}}$
- $P_{t,\mu^+\mu^-}, \cos\theta_{\mu^+\mu^-}, \cos\theta_h$
- charge \*  $\cos\theta_{\mu^-}, \text{charge} * \cos\theta_{\mu^+}$
- $M_{\text{rec}}$

The following figures are the distributions of each input variable. All histograms are normalized to 1. Blue shows signal and red shows background.


 Figure 22:  $E_{\text{vis}}$  distribution.

 Figure 23:  $\cos\theta_{\text{thrust}}$  distribution.

 Figure 24:  $P_{t,\mu^+\mu^-}$  distribution.

 Figure 25:  $\cos\theta_{\mu^+\mu^-}$  distribution.

 Figure 26:  $\cos\theta_h$  distribution.

 Figure 27: charge \*  $\cos\theta_{\mu^-}$  distribution.

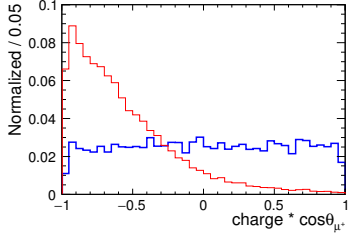


Figure 28: charge \*  $\cos\theta_{\mu^+}$  distribution.

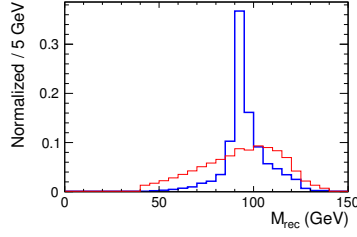


Figure 29:  $M_{\text{rec}}$  distribution.

The next figure shows the result of TMVA analysis. I decided a cut as BDTG output  $> 0.6$ .

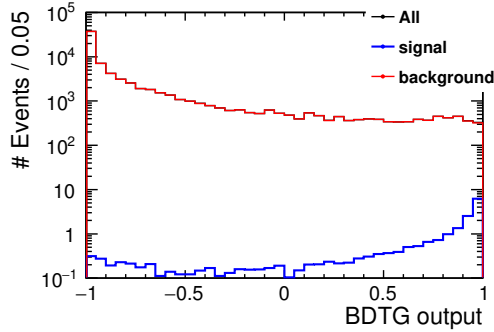


Figure 30: BDTG output distribution.

## 2.5 Toy MC Study

The next figure shows the  $M_{\mu^+\mu^-}$  distribution after BDTG output cut.

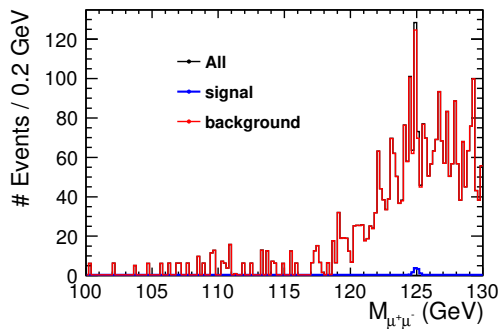


Figure 31:  $M_{\mu^+\mu^-}$  distribution.

I applied further cut of  $M_{\mu^+\mu^-} > 120$  GeV. The number of events after all cuts were  $N_S = 13$  and  $N_B = 2704$ . I used a normalized Gaussian (gausn) for signal modeling and a constant (pol0) for background modeling. The next figure shows the result of fitting. Signal is green and background is yellow. I used log-likelihood method for the background fitting.

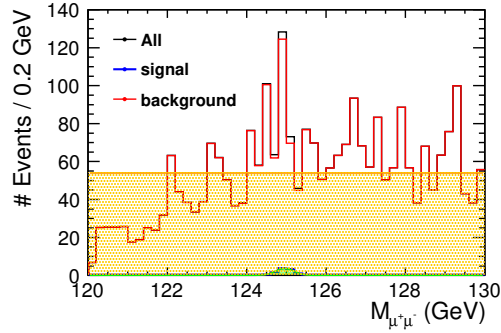


Figure 32: Fitting result of  $M_{\mu^+\mu^-}$ .

Now I got model functions, I will perform pseudo-experiment. The next figure shows one example of fitting. Blue shows signal pseudo-data, red shows background pseudo-data, black is blue plus red, and purple curve shows the result of fitting with function  $f$ .

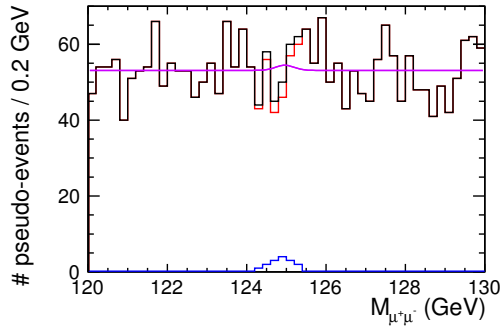


Figure 33: Example of one pseudo-experiment.

I performed 200000 pseudo-experiments. The next 2 figures show the obtained  $Y_S$  distribution and pull distribution.

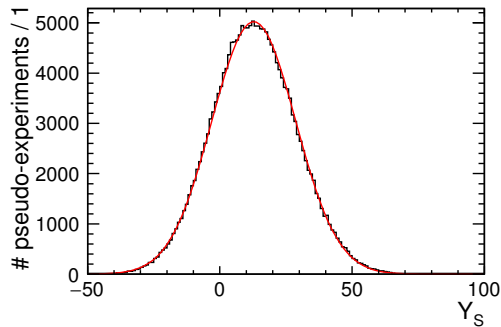


Figure 34:  $Y_S$  distribution.

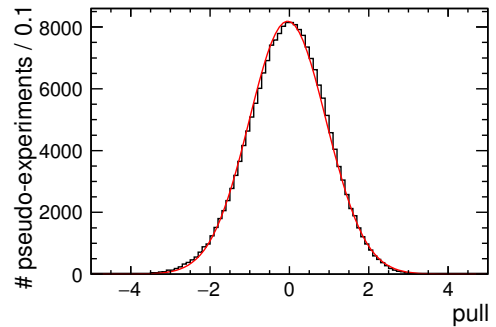


Figure 35: Pull distribution.

The Gaussian fit to  $Y_S$  distribution returned the mean of  $12.851 \pm 0.036$  and the width of  $15.868 \pm 0.025$ . The resulting precision was calculated to be 123.5%. The Gaussian fit to pull distribution returned the mean of  $-0.0414 \pm 0.0022$  and the width of  $0.9711 \pm 0.0015$ .



### 3 250 GeV $e^+e^- \rightarrow \nu\bar{\nu}h$ analysis: right-handed (nnh250-R)

#### 3.1 MC Sample

Of course I used same samples used in other 250 GeV analysis.

#### 3.2 Event Reconstruction

I applied same event reconstruction method which used at nnh250-L analysis.

#### 3.3 Precuts

I applied same precuts used at nnh250-L analysis. Following figures are the distributions of each variable and the table is cut table.

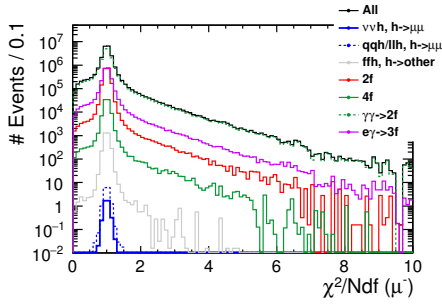


Figure 36:  $\chi^2/Ndf(\mu^-)$  distribution.

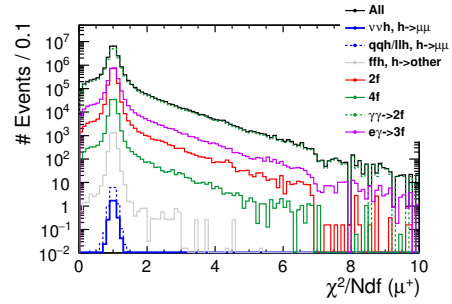


Figure 37:  $\chi^2/Ndf(\mu^+)$  distribution.

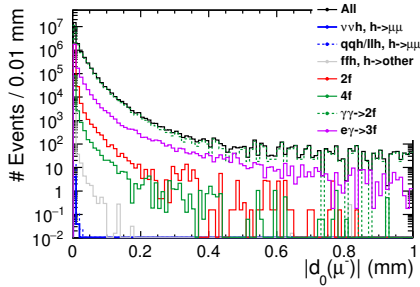


Figure 38:  $|d_0(\mu^-)|$  distribution.

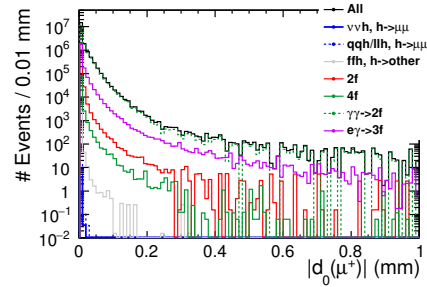


Figure 39:  $|d_0(\mu^+)|$  distribution.

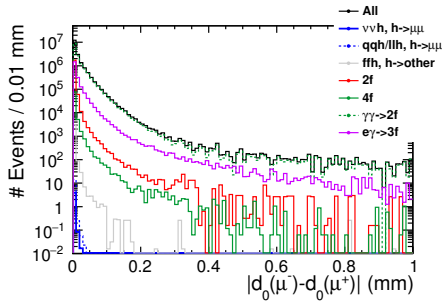


Figure 40:  $|d_0(\mu^-) - d_0(\mu^+)|$  distribution.

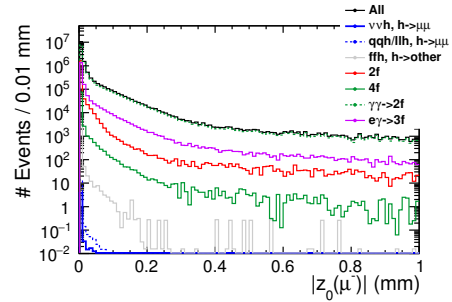


Figure 41:  $|z_0(\mu^-)|$  distribution.

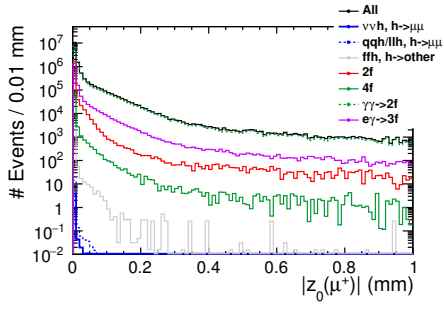


Figure 42:  $|z_0(\mu^+)|$  distribution.

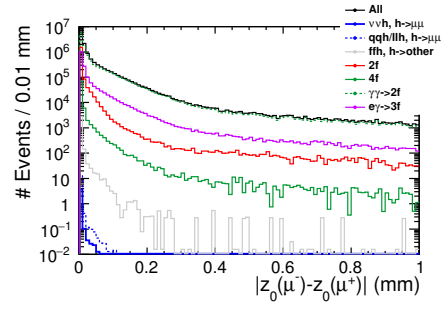


Figure 43:  $|z_0(\mu^-) - z_0(\mu^+)|$  distribution.

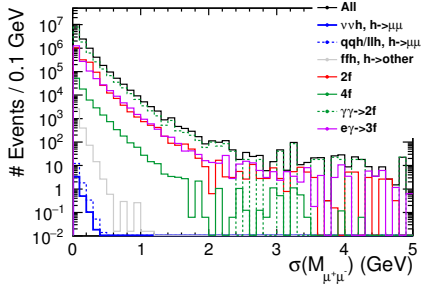


Figure 44:  $\sigma(M_{\mu^+\mu^-})$  distribution.

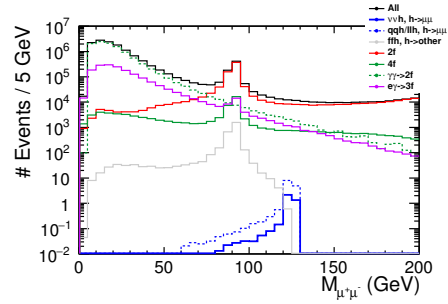


Figure 45:  $M_{\mu^+\mu^-}$  distribution.

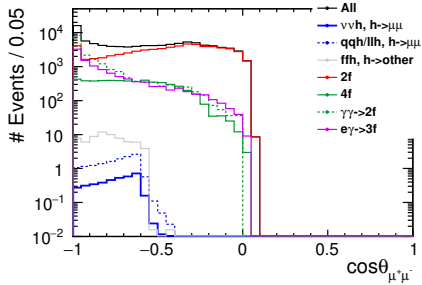


Figure 46:  $\cos \theta_{\mu^+\mu^-}$  distribution.

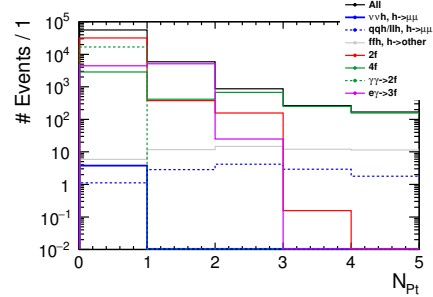


Figure 47:  $N_{P_t > 5\text{GeV}}$  distribution.

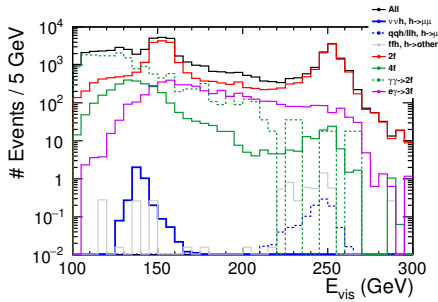


Figure 48:  $E_{\text{vis}}$  distribution.

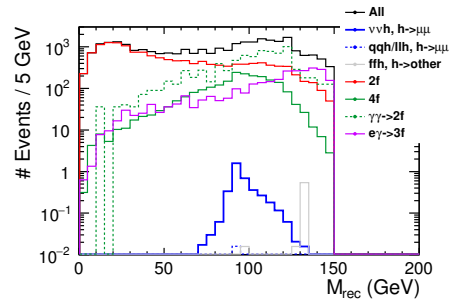


Figure 49:  $M_{\text{rec}}$  distribution.

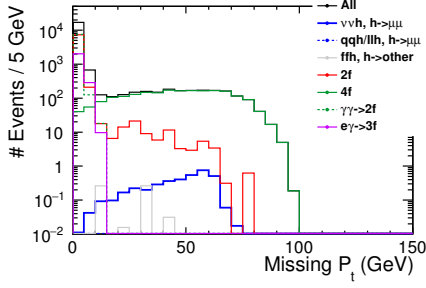


Figure 50: Missing  $P_t$  distribution.

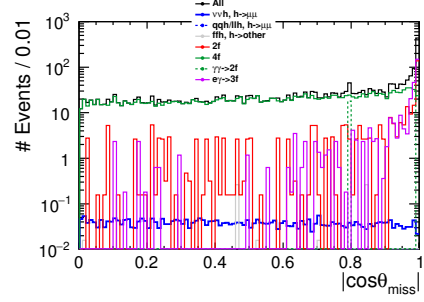


Figure 51:  $|\cos \theta_{\text{miss}}|$  distribution.

Table 2: Cut table of nnh250-R at the precuts.

	$\nu\nu h$ $h \rightarrow \mu\mu$	$qqh+\ell\ell h$ $h \rightarrow \mu\mu$	$ffh$ $h \rightarrow \text{other}$	2f	4f	$\gamma\gamma \rightarrow 2f$	3f
No cut	4.19	16.22	$9.266 \times 10^4$	$3.654 \times 10^7$	$2.295 \times 10^6$	$2.975 \times 10^8$	$6.821 \times 10^8$
$\# \mu^\pm$	4.03	14.74	3178.03	$1.845 \times 10^6$	$9.065 \times 10^4$	$1.800 \times 10^7$	$2.412 \times 10^6$
$\chi^2/\text{Ndf}$	3.98	14.60	3140.65	$1.785 \times 10^6$	$8.613 \times 10^4$	$1.492 \times 10^7$	$2.110 \times 10^6$
$d_0$	3.96	14.49	3090.25	$1.760 \times 10^6$	$8.221 \times 10^4$	$1.103 \times 10^7$	$1.750 \times 10^6$
$z_0$	3.95	14.48	3087.29	$1.756 \times 10^6$	$8.197 \times 10^4$	$1.088 \times 10^7$	$1.732 \times 10^6$
$\sigma(M_{\mu\mu})$	3.95	14.47	3086.07	$1.718 \times 10^6$	$8.047 \times 10^4$	$1.072 \times 10^7$	$1.696 \times 10^6$
$M_{\mu\mu}$	3.82	14.05	68.12	$6.429 \times 10^4$	5261.76	$1.787 \times 10^4$	$1.063 \times 10^4$
$\cos \theta_{\mu\mu}$	3.81	14.03	68.12	$3.228 \times 10^4$	4456.24	$1.686 \times 10^4$	9617.56
$N_{P_t}$	3.80	1.12	5.89	$3.174 \times 10^4$	2846.20	$1.686 \times 10^4$	4461.30
$E_{\text{vis}}$	3.79	0.03	0.57	$1.829 \times 10^4$	2169.39	8129.69	2900.79
$M_{\text{rec}}$	3.79	0.03	0.57	7615.86	2073.90	7621.58	2326.83
missing	3.78	0.03	0.57	311.16	2033.52	143.89	296.92
$\theta_{\text{miss}}$	3.75	0.03	0.57	173.66	2009.83	17.99	147.02

### 3.4 TMVA Analysis

I used same variables used at nnh250-L analysis as the inputs to TMVA. The following figures are the distributions of each input variable. All histograms are normalized to 1. Blue shows signal and red shows background.

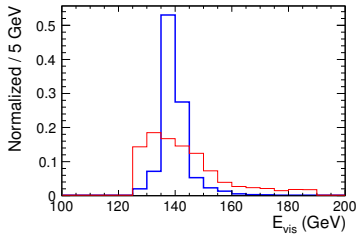


Figure 52:  $E_{\text{vis}}$  distribution.

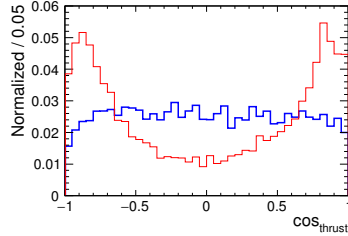


Figure 53:  $\cos \theta_{\text{thrust}}$  distribution.

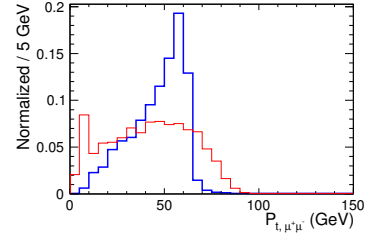


Figure 54:  $P_{t, \mu^+ \mu^-}$  distribution.

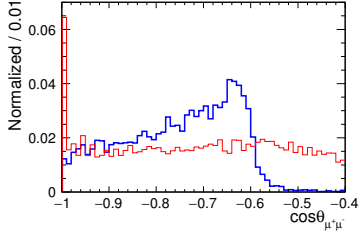


Figure 55:  $\cos \theta_{\mu^+\mu^-}$  distribution.

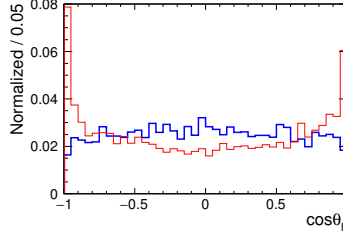


Figure 56:  $\cos \theta_h$  distribution.

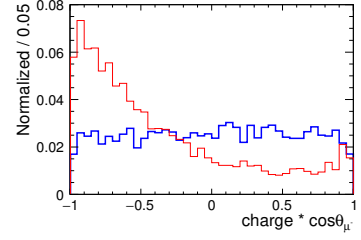


Figure 57: charge \*  $\cos \theta_{\mu^-}$  distribution.

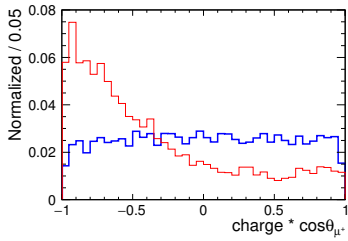


Figure 58: charge \*  $\cos \theta_{\mu^+}$  distribution.

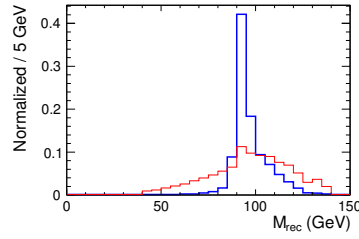


Figure 59:  $M_{\text{rec}}$  distribution.

The next figure shows the result of TMVA analysis. I decided a cut as BDTG output  $> 0.3$ .

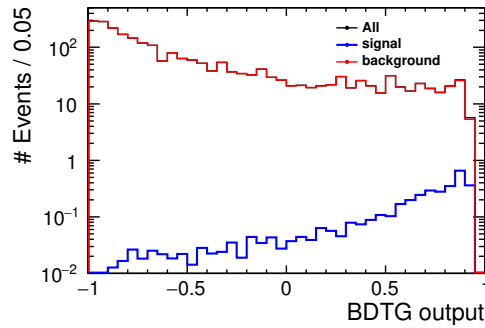


Figure 60: BDTG output distribution.

### 3.5 Toy MC Study

The next figure shows the  $M_{\mu^+\mu^-}$  distribution after BDTG output cut.

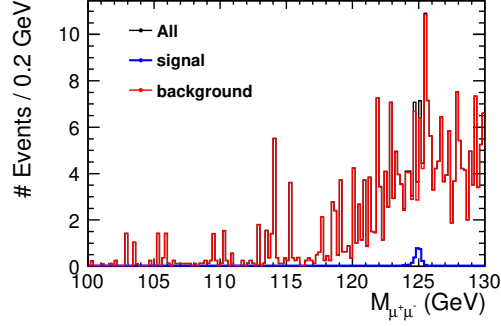


Figure 61:  $M_{\mu^+\mu^-}$  distribution.

I applied further cut of  $M_{\mu^+\mu^-} > 120$  GeV. The number of events after all cuts were  $N_S = 4$  and  $N_B = 210$ . I used a normalized Gaussian (gauss) for signal modeling and a constant (pol0) for background modeling. The next figure shows the result of fitting. Signal is green and background is yellow. I used log-likelihood method to perform the fitting for background.

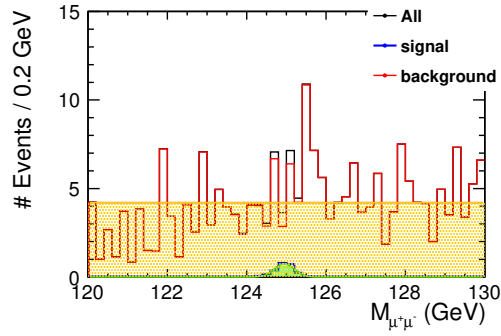


Figure 62: Fitting result of  $M_{\mu^+\mu^-}$

Now I got model functions, I will perform pseudo-experiment. The next figure shows one example of fitting. Blue shows signal pseudo-data, red shows background pseudo-data, black is blue plus red, and purple curve shows the result of fitting with function  $f$ .

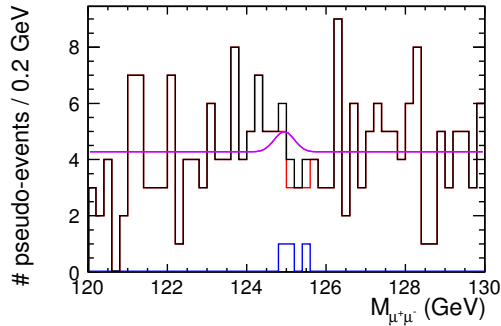


Figure 63: Example of one pseudo-experiment.

I performed 200000 pseudo-experiments. The next 2 figures show the obtained  $Y_S$  distribution and pull distribution.

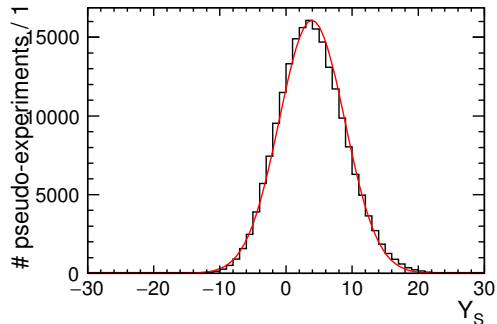


Figure 64:  $Y_S$  distribution.

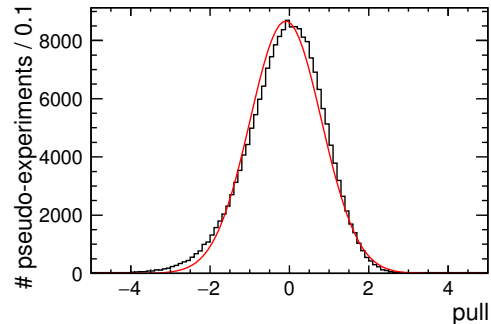


Figure 65: Pull distribution.

The Gaussian fit to  $Y_S$  distribution returned the mean of  $3.927 \pm 0.012$  and the width of  $4.9255 \pm 0.0077$ . The resulting precision was calculated to be 125.4%. The Gaussian fit to pull distribution returned the mean of  $-0.0888 \pm 0.0022$  and the width of  $0.9008 \pm 0.0014$ .

## 4 Summary and Prospects

Next table shows the summary of results.

Table 3: Summary of the precision  $\frac{\Delta(\sigma \times \text{BR})}{(\sigma \times \text{BR})}$ .

500 GeV	$q\bar{q}h$	$\nu\bar{\nu}h$
left-handed	47.8% (1600 fb $^{-1}$ )	39.2% (1600 fb $^{-1}$ )
right-handed	52.1% (1600 fb $^{-1}$ )	71.5% (1600 fb $^{-1}$ )
250 GeV	$q\bar{q}h$	$\nu\bar{\nu}h$
left-handed	30.0% (1350 fb $^{-1}$ )	123.5% (1350 fb $^{-1}$ )
right-handed	52.5% (450 fb $^{-1}$ )	125.4% (450 fb $^{-1}$ )

Even I have limited MC statistics, I obtained reliable numbers by using toy MC. But the precision for all channels get worse. The previous results were too good. Combined precision is calculate to be 17.5%. HL-LHC with 3000 fb $^{-1}$  case gives 14% precision, so that my result is relatively 25% worse.

The pull distribution after toy MC study was a bit asymmetric. The possible reasons are:

- not suitable fitting using Gaussian to the  $Y_S$  distribution with average  $\sim 10$ .
- normalized Gaussian is not a suitable fitting function for  $M_{\mu^+\mu^-}$  because it has a tail in low mass region due to FSR.

The remaining tasks are:

- how to handle SGV [12] samples.
- re-weighting.

## References

- [1] Shin-ichi Kawada “An analysis of  $h \rightarrow \mu^+\mu^-$  mode at the center-of-mass energy of 500 GeV ILC”
- [2] Shin-ichi Kawada “An analysis of  $h \rightarrow \mu^+\mu^-$  mode at the center-of-mass energy of 500 GeV ILC — part 2”

- [3] Shin-ichi Kawada “An analysis of  $h \rightarrow \mu^+\mu^-$  mode at the center-of-mass energy of 500 GeV ILC — part 3”
- [4] Shin-ichi Kawada “An analysis of  $h \rightarrow \mu^+\mu^-$  mode at the center-of-mass energy of 500 GeV ILC — part 4”
- [5] Shin-ichi Kawada “An analysis of  $h \rightarrow \mu^+\mu^-$  mode at the center-of-mass energy of 500 GeV ILC — part 5”
- [6] Shin-ichi Kawada “An analysis of  $h \rightarrow \mu^+\mu^-$  mode at the center-of-mass energy of 500 GeV ILC — part 6”
- [7] Shin-ichi Kawada “An analysis of  $h \rightarrow \mu^+\mu^-$  mode at the center-of-mass energy of 250/500 GeV ILC — part 7”
- [8] Shin-ichi Kawada “An analysis of  $h \rightarrow \mu^+\mu^-$  mode at the center-of-mass energy of 250/500 GeV ILC — part 8”
- [9] <https://ild.ngt.ndu.ac.jp/eelog/dbd-prod/>
- [10] Junping Tian, Claude Dürig “isolated lepton finder”  
[https://agenda.linearcollider.org/event/6787/contributions/33415/  
attachments/27509/41775/IsoLep\\_HLRec2016.pdf](https://agenda.linearcollider.org/event/6787/contributions/33415/attachments/27509/41775/IsoLep_HLRec2016.pdf)
- [11] S. Catani, Yu. L. Dokshitzer, M. Olsson, G. Turnock, B. R. Webber, “New clustering algorithm for multijet cross sections in  $e^+e^-$  annihilation”, Phys. Lett. B **269** (1991) 432 - 438
- [12] Mikael Berggren, “SGV 3.0 — a fast detector simulation”, arXiv:1203.0217 [physics.ins-det] (2012)